
This is an electronic reprint of the original article.
This reprint may differ from the original in pagination and typographic detail.

Tang, Mengxue; Vehkapera, Mikko; Chu, Xiaoli; Wichman, Risto

Power allocation for multipair massive MIMO FD relay systems with low resolution ADCs

Published in:

ISWCS 2019 - 16th International Symposium on Wireless Communication Systems

DOI:

[10.1109/ISWCS.2019.8877176](https://doi.org/10.1109/ISWCS.2019.8877176)

Published: 01/08/2019

Document Version

Peer-reviewed accepted author manuscript, also known as Final accepted manuscript or Post-print

Please cite the original version:

Tang, M., Vehkapera, M., Chu, X., & Wichman, R. (2019). Power allocation for multipair massive MIMO FD relay systems with low resolution ADCs. In *ISWCS 2019 - 16th International Symposium on Wireless Communication Systems* (pp. 505-510). Article 8877176 (International Symposium on Wireless Communication Systems). IEEE. <https://doi.org/10.1109/ISWCS.2019.8877176>

This material is protected by copyright and other intellectual property rights, and duplication or sale of all or part of any of the repository collections is not permitted, except that material may be duplicated by you for your research use or educational purposes in electronic or print form. You must obtain permission for any other use. Electronic or print copies may not be offered, whether for sale or otherwise to anyone who is not an authorised user.

Power Allocation for Multipair Massive MIMO FD Relay Systems with Low Resolution ADCs

Mengxue Tang*, Mikko Vehkaperä†, Xiaoli Chu* and Risto Wichman†

*Department of Electronic and Electrical Engineering, University of Sheffield, Sheffield, UK

†Department of Signal Processing and Acoustics, Aalto University School of Electrical Engineering, Finland

Email: {mtang11, x.chu}@sheffield.ac.uk and {mikko.vehkaperä, risto.wichman}@aalto.fi

Abstract—To reduce energy consumption, relay stations with massive antenna arrays can be equipped with low resolution analog-to-digital converters (ADCs). Due to powerful loop interference in full-duplex (FD) relaying, however, low resolution ADCs generate strong quantization noise that has severe impact on the throughput of the system. In this paper, the throughput and energy efficiency of a FD decode-and-forward relay system with low resolution ADCs is investigated. Based on the mathematical analysis, a novel iterative power allocation scheme that mitigates the impact of the quantization noise via reducing the received LI power is proposed. The power allocation scheme aims at maximizing the end-to-end achievable rate by adjusting the per-link transmit powers at the relay. The numerical results show that compared to half-duplex relaying, using FD with the proposed power allocation scheme improves the system throughput and energy efficiency significantly.

Index Terms—full-duplex relaying, low resolution ADCs, power allocation, massive MIMO, decode-and-forward, energy efficiency, finite code word length.

I. INTRODUCTION

Full-duplex (FD) relaying is known to outperform half-duplex (HD) relaying if the loop interference (LI) caused by simultaneous transmission and reception can be mitigated to the level of thermal noise before detection and decoding [1]–[7]. A combination of passive isolation of antennas, analog circuit domain cancellation and LI cancellation in baseband are typically required to reach the desired attenuation [2], [4]. In addition, massive antenna arrays at the relay can be employed to mitigate the LI and reduce inter-user interference in multipair relaying systems [3], [5], [6]. One of the main drawbacks of using large-scale antenna arrays is increased energy consumption that affects the energy efficiency (EE) of the system. In particular, the power consumed by analog-to-digital converters (ADCs) at a fully digital relay receiver grows linearly with the number of antennas and can be a major factor for systems with large number of antennas [8], [9].

Compared to full resolution ADCs, low resolution ADCs consume less power, have smaller area occupation on chips and are cheaper [8], [10]. The use of low resolution ADCs in multiple-input multiple-output (MIMO) systems has been investigated in several works; see for example [11], [12]. To the best of our knowledge, however, the research in massive

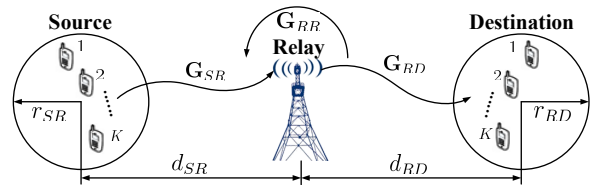


Fig. 1. Multipair full-duplex relaying system.

MIMO FD relaying with low resolution ADCs is limited to the case of amplify-and-forward mode, where the residual LI is assumed to be weak and independent of the quantization noise [13]. This assumption is reasonable if ideal hardware with full resolution ADCs is employed so that both analog and digital domain LI mitigation techniques can be used. With low resolution ADCs, however, the power of the quantization noise scales with the power of the received signal after passive isolation and analog circuit domain cancellation [4], [14]. Since the power of residual LI at this stage is high, the quantization noise has severe impact on the performance.

In this paper, the throughput and energy efficiency of a multipair full-duplex DF relaying system (see Fig. 1) that suffers from realistic levels of residual LI after passive and analog cancellation is investigated. Based on the mathematical analysis, we develop an iterative power allocation scheme that controls the link-wise transmit powers at the relay by taking into account the resolution of the ADCs and the transmit-side hardware impairments. The proposed scheme is based on an extension of our previous work [15] where full resolution ADCs were employed at the relay. By reducing the effects of quantization noise and residual LI in the system, the power allocation algorithm aims at maximizing the pairwise end-to-end (E2E) achievable rate. The proposed scheme uses statistical information, so that instantaneous channel state information (CSI) is not needed and the power allocation update frequency is low. In addition, we carry out detailed EE investigation and in the spirit of ultra-reliable and low-latency communications (URLLC) [16], examine the effects of imposing strict delay constraint, i.e., finite code word length, on the system. The numerical results show that compared to HD relaying, the proposed FD transmission scheme provides significant gains in system throughput and energy efficiency in both delay sensitive and insensitive cases.

II. SYSTEM MODEL

The multipair relaying system considered in the present work is depicted in Fig. 1. A decode-and-forward FD massive MIMO relay with M_t transmit and M_r receive antennas is used to establish the connections between K source-destination pairs. The direct links between the source and destination terminals are assumed to be blocked. The terminals are equipped with one antenna and they operate in HD mode. For simplicity, we assume that the source and destination terminals are located inside circles that are d_{SR} and d_{RD} meters away from the relay, respectively. The radiuses (in meters) of the circles are denoted as r_{SR} and r_{RD} , respectively.

The source-to-relay, \mathbf{G}_{SR} , and relay-to-destination, \mathbf{G}_{RD}^T , channel matrices take into account both fast fading and large scale attenuation. We write¹ $\mathbf{G}_* = \mathbf{H}_* \mathbf{D}_*^{1/2}$, where the entries of \mathbf{H}_* are i.i.d. standard circularly symmetric complex Gaussian (CSCG) and \mathbf{D}_* is a diagonal matrix whose k th diagonal entry $\beta_{*,k}$ models path loss and shadowing between the k th terminal and the relay. We assume that the relay knows the channel statistics \mathbf{D}_{SR} and \mathbf{D}_{RD} perfectly, but needs to estimate the instantaneous CSI represented by the matrices \mathbf{H}_{SR} and \mathbf{H}_{RD} . Since passive and analog cancellation schemes are used to mitigate the direct path of the LI channel, the elements of the LI channel matrix \mathbf{G}_{RR} are assumed to be i.i.d. CSCG with variance β_R [2]. As the coherence time of the LI channel is typically much longer than that of the S→R and R→D channels [17, Table I], we assume that the relay station can estimate the LI channel accurately, with negligible loss in throughput [15].

The received signals at the relay and destination terminals are given by [3], [5], [18]

$$\mathbf{y}_R = \mathbf{G}_{SR} \mathbf{x}_S[i] + \mathbf{G}_{RR} \mathbf{x}_R[i] + \mathbf{G}_{RR} \mathbf{u}_t + \mathbf{n}'_R, \quad (1)$$

$$\mathbf{y}_D = \mathbf{G}_{RD}^T (\mathbf{x}_R[i] + \mathbf{u}_t) + \mathbf{n}_D, \quad (2)$$

where \mathbf{y}_R denotes the signal after analog circuit domain cancellation before ADCs. The signals transmitted by the sources and the relay at time instant i are $\mathbf{x}_S[i] \in \mathbb{C}^K$ and $\mathbf{x}_R[i] \in \mathbb{C}^{M_t}$, respectively. The elements of the thermal noise vectors \mathbf{n}'_R and \mathbf{n}_D are i.i.d. $\mathcal{CN}(0, \sigma_w^2)$. The transmit-side noise vector $\mathbf{u}_t \sim \mathcal{CN}(\mathbf{0}, \mu_t \text{diag}(\mathbb{E}\{\mathbf{x}_R \mathbf{x}_R^H\}))$ takes into account the combined effects of hardware impairments at the transmit-side of the relay, where the coefficient $\mu_t > 0$ is related to the error vector magnitude (EVM) requirements of the system [5], [18]. In the following, we omit \mathbf{u}_t from the R→D link since it has negligible impact on the rate. To focus on the impact of quantization noise due to low resolution ADCs, we do not consider other receive-side imperfection (such as I/Q imbalance) in this paper. Such effects can be incorporated in the system model e.g. as done in [15] if desired. Since the source and destination terminals have only one antenna, they are assumed to be equipped with ideal hardware, including full resolution ADCs.

¹Whenever * is used, the actual subscript can be inferred from the context.

TABLE I
 θ FOR DIFFERENT RESOLUTIONS OF ADCs

N	1	2	3	4	5	≥ 6
θ	0.6366	0.8825	0.96546	0.990503	0.997501	$1 - \frac{\pi\sqrt{3}}{2} 2^{-2N}$

A. Quantization with Low-resolution ADCs

At the receive-side of the relay station, low-resolution ADCs are assumed to be used for energy saving purposes. We model the quantized received signal as [14], [19]

$$\begin{aligned} \tilde{\mathbf{y}}_R &= \theta \mathbf{y}_R + \mathbf{n}_q \\ &= \theta \mathbf{G}_{SR} \mathbf{x}_S[i] + \theta \mathbf{G}_{RR} \mathbf{x}_R[i] + \underbrace{\theta \mathbf{G}_{RR} \mathbf{u}_t + \theta \mathbf{n}'_R}_{\triangleq \mathbf{n}_R} + \mathbf{n}_q. \end{aligned} \quad (3)$$

The quantization noise is modeled as a CSCG vector $\mathbf{n}_q \sim \mathcal{CN}(\mathbf{0}, \theta(1-\theta) \text{diag}(\mathbb{E}\{\mathbf{y}_R \mathbf{y}_R^H\}))$ that is assumed to be independent of the received signal (1). Note that since the covariance matrix of \mathbf{n}_q depends on the statistics of the received signal after analog circuit domain cancellation, digital baseband LI cancellation cannot be used to reduce the level of quantization noise in the system. The coefficient $\theta > 0$ is related to the resolution N of the ADCs and Table I lists the values of θ for different choices of N [8]. For notational convenience, we combine the terms related to transmit-side noise, quantization noise and thermal noise as one term \mathbf{n}_R as shown in (3). Note that \mathbf{n}_R neither is Gaussian distributed nor has i.i.d. elements in general.

B. Channel Estimation

Block fading with a coherence time of T symbols is assumed for the channels between the terminals and the relay. To facilitate channel estimation, the source and destination terminals transmit pilot matrices Φ_S and Φ_D , respectively, at the beginning of each coherence block. To satisfy pilot orthogonality, we let Φ_S and Φ_D be $K \times K$ diagonal matrices with $\sqrt{K\rho_{pS,k}}$ and $\sqrt{K\rho_{pD,k}}$ as the k th diagonal entry, respectively. The received pilots at the relay station after ADCs are given by

$$\begin{aligned} \tilde{\mathbf{Y}}_{SR} &= \theta \mathbf{G}_{SR} \Phi_S + \mathbf{N}_{SR}, \\ \tilde{\mathbf{Y}}_{DR} &= \theta \mathbf{G}_{RD} \Phi_D + \mathbf{N}_{DR}, \end{aligned}$$

where the additive noise matrices model the combination of quantization and thermal noise. The entries of \mathbf{N}_{SR} and \mathbf{N}_{DR} are assumed to be independent CSCG and the variance of the elements on the k th column are

$$\begin{aligned} \sigma_{SR,k}^2 &= \theta(1-\theta)K\rho_{pS,k}\beta_{SR,k} + \theta\sigma_w^2, \\ \sigma_{RD,k}^2 &= \theta(1-\theta)K\rho_{pD,k}\beta_{RD,k} + \theta\sigma_w^2, \end{aligned}$$

respectively.

After receiving the pilots from the terminals, the relay calculates the channel estimates $\hat{\mathbf{G}}_{SR}$ and $\hat{\mathbf{G}}_{RD}$. We denote $\hat{\mathbf{G}}_* = \mathbf{G}_* - \hat{\mathbf{G}}_*$ for the error matrix and assume linear minimum mean squared error (LMMSE) estimator is used to obtain the CSI. As a result, the estimates and the errors are uncorrelated [20]. For the system under investigation, the

entries in the k th column of $\tilde{\mathbf{G}}_{\text{SR}}$ and $\tilde{\mathbf{G}}_{\text{RD}}$ with LMMSE estimation are independent CSCG with variance [8], [15]

$$\tilde{\beta}_{\text{SR},k} = \frac{(1-\theta)K\rho_{\text{pS},k}\beta_{\text{SR},k}^2 + \sigma_{\text{w}}^2\beta_{\text{SR},k}}{K\rho_{\text{pS},k}\beta_{\text{SR},k} + \sigma_{\text{w}}^2},$$

$$\tilde{\beta}_{\text{RD},k} = \frac{(1-\theta)K\rho_{\text{pD},k}\beta_{\text{SR},k}^2 + \sigma_{\text{w}}^2\beta_{\text{SR},k}}{K\rho_{\text{pD},k}\beta_{\text{RD},k} + \sigma_{\text{w}}^2},$$

respectively. The properties of the estimator also guarantee that $\hat{\beta}_* = \beta_* - \tilde{\beta}_*$ holds for all channels.

As mentioned earlier in the paper, the coherence time of the LI channel is typically much longer than that of the S→R and R→D channels [17, Table I]. Therefore, we assume that the relay has perfect knowledge of the LI channel \mathbf{G}_{RR} .

C. Data Transmission

For notational convenience, we write the transmit signals from the source terminals at time instant i as

$$\mathbf{x}_{\text{S}}[i] = \text{diag}(\sqrt{\rho_{\text{S},1}}, \sqrt{\rho_{\text{S},2}}, \dots, \sqrt{\rho_{\text{S},K}})\mathbf{m}[i],$$

where the entries of $\mathbf{m}[i]$ are i.i.d. standard CSCG. After subtracting the known part of the LI from the quantized signal (3) by using the knowledge of θ , \mathbf{G}_{RR} and $\mathbf{x}_{\text{R}}[i]$, the receive-side signal at the relay is given by

$$\theta\mathbf{G}_{\text{SR}}\mathbf{x}_{\text{S}}[i] + \mathbf{n}_{\text{R}} = \tilde{\mathbf{y}}_{\text{R}}[i] - \theta\mathbf{G}_{\text{RR}}\mathbf{x}_{\text{R}}[i].$$

Note that although the data-dependent part of the LI is perfectly cancelled in baseband, the transmit-side noise received through the LI channel as well as the quantization noise can still have severe impact on the performance of the system via \mathbf{n}_{R} . The power of the noise term \mathbf{n}_{R} , defined in (3), will be calculated in the next section.

After ADCs, the relay uses linear estimator \mathbf{W} to separate the data streams transmitted by the source terminals. The k th estimated signal stream at the relay reads then

$$z_{\text{R},k}[i] = \theta\mathbf{w}_k^H \mathbf{g}_{\text{SR},k} x_{\text{S},k}[i] + \theta \sum_{j \neq k} \mathbf{w}_k^H \mathbf{g}_{\text{SR},j} x_{\text{S},j}[i] + \mathbf{w}_k^H \mathbf{n}_{\text{R}}, \quad (4)$$

where $\mathbf{g}_{\text{SR},k}$, $\mathbf{g}_{\text{RR},k}$ and \mathbf{w}_k are the k th columns of \mathbf{G}_{SR} , \mathbf{G}_{RR} and \mathbf{W} , respectively, and $x_{\text{S},k}[i]$ is the k th element of $\mathbf{x}_{\text{S}}[i]$. Similarly, linear precoding with matrix \mathbf{A} is used at the relay to transmit the data to the destination terminals, where the received signal at the k th terminal reads

$$y_{\text{D},k}[i] = \mathbf{g}_{\text{RD},k}^T \mathbf{a}_k m_k[i - \tau] + \sum_{j \neq k} \mathbf{g}_{\text{RD},k}^T \mathbf{a}_j m_j[i - \tau] + n_{\text{D},k}.$$

Here $\mathbf{g}_{\text{RD},k}$, \mathbf{a}_k , $m_k[i - \tau]$ and $n_{\text{D},k}$ denote the k th columns (or elements) of \mathbf{G}_{RD} , \mathbf{A} , $\mathbf{m}[i - \tau]$ and \mathbf{n}_{D} , respectively. We assume that in DF relaying the decoding delay is $\tau \geq 1$ symbols so that $\mathbf{x}_{\text{R}}[i] = \mathbf{A}\mathbf{m}[i - \tau]$ and, thus, the transmitted signal is uncorrelated with the received signal at the relay [1]. Finally, note that the estimation and precoding matrices \mathbf{W} and \mathbf{A} are functions of $\hat{\mathbf{G}}_{\text{SR}}$ and $\hat{\mathbf{G}}_{\text{RD}}$, respectively.

III. ACHIEVABLE RATE ANALYSIS

Since \mathbf{n}_{R} is not Gaussian distributed, we resort to calculating a lower bound on the achievable rate by replacing the combination of inter-pair interference and noise in (4) by a CSCG term that has the same variance but is independent of the desired signal [21]. For the k th S→R and R→D links, the lower bounds² on achievable rates are given by

$$R_{*,k} = \log_2(1 + \text{SINR}_{*,k}). \quad (5)$$

The signal-to-interference-plus-noise ratios associated with (5) are given in (6) and (7) at the top of the next page, where \mathbf{n}_{R} denotes—with some abuse of notation—a CSCG vector that is independent of the desired signal and has i.i.d. entries of variance (provided later in this section) σ_{R}^2 .

To calculate a lower bound on the ergodic E2E rate R_k for the k th terminal pair, we follow [3] and let

$$R_k = \min\{R_{\text{SR},k}, R_{\text{RD},k}\} \\ = \log_2(1 + \min\{\text{SINR}_{\text{SR},k}, \text{SINR}_{\text{RD},k}\}). \quad (8)$$

Due to space constraints, we limit our analysis to zero-forcing (ZF) processing for both estimation and precoding, so that

$$\mathbf{W}^H = (\hat{\mathbf{G}}_{\text{SR}}^H \hat{\mathbf{G}}_{\text{SR}})^{-1} \hat{\mathbf{G}}_{\text{SR}}^H, \\ \mathbf{A} = \mathbf{B}\mathbf{P} = \hat{\mathbf{G}}_{\text{RD}}^* (\hat{\mathbf{G}}_{\text{RD}}^T \hat{\mathbf{G}}_{\text{RD}}^*)^{-1} \mathbf{P},$$

where $\mathbf{P} \in \mathbb{C}^{K \times K}$ is a power allocation matrix. The k th diagonal entry of \mathbf{P} is given by

$$p_k = \sqrt{\frac{q_k}{\mathbb{E}\{\|\mathbf{b}_k\|^2\}}} = \sqrt{(M_t - K)\hat{\beta}_{\text{RD},k} q_k},$$

where \mathbf{b}_k is the k th column of \mathbf{B} and q_k denotes the relay's transmit power for the k th link. The q_k 's that maximize the pairwise E2E rate are designed in the next section.

Using similar techniques as in [15], a lower bound for the E2E achievable rate of the k th terminal pair reads

$$R_k = \log_2 \left(1 + \min \left(\frac{\theta^2 \rho_{\text{S},k} (M_t - K) \hat{\beta}_{\text{SR},k}}{\theta^2 \sum_{j=1}^K \rho_{\text{S},j} \tilde{\beta}_{\text{SR},j} + \sigma_{\text{R}}^2}, \right. \right. \\ \left. \left. \frac{(M_t - K) \hat{\beta}_{\text{RD},k} q_k}{\hat{\beta}_{\text{RD},k} q_{\text{tot}} + \sigma_{\text{w}}^2} \right) \right), \quad (9)$$

where $q_{\text{tot}} = \sum_k q_k$ is the total transmit power of the relay. The variance of the elements of \mathbf{n}_{R} is given by

$$\sigma_{\text{R}}^2 = \theta \mu_t \beta_{\text{R}} q_{\text{tot}} + \theta(1-\theta) \left(\sum_{k=1}^K \rho_{\text{S},k} \beta_{\text{SR},k} + \beta_{\text{R}} q_{\text{tot}} \right) + \theta \sigma_{\text{w}}^2.$$

Given the above achievable rate analysis, we define the average E2E throughput as

$$C = f_{\text{B}} \cdot \frac{T - 2K}{T} \cdot \mathbb{E} \left\{ \sum_{k=1}^K R_k \right\}, \quad (10)$$

where f_{B} denotes the system bandwidth. Note that the expectation in (10) is over the terminal locations and shadowing.

²Although the relay has instantaneous channel estimates $\hat{\mathbf{g}}_{\text{SR},k}$, as in [3], [5], we assume that statistical channel estimates $\mathbb{E}_{\{\mathbf{g}\}}\{\mathbf{w}_k^H \hat{\mathbf{g}}_{\text{SR},k}\}$ are used for decoding. This provides a lower bound on the SINR of the S→R link.

$$\text{SINR}_{\text{SR},k} = \frac{\rho_{\text{S},k} |\mathbb{E}_{\{\mathbf{g}\}} \{\mathbf{w}_k^H \mathbf{g}_{\text{SR},k}\}|^2}{\rho_{\text{S},k} \text{Var}_{\{\mathbf{g}\}} (\mathbf{w}_k^H \mathbf{g}_{\text{SR},k}) + \sum_{j=1, j \neq k}^K \rho_{\text{S},j} \mathbb{E}_{\{\mathbf{g}\}} \{|\mathbf{w}_k^H \mathbf{g}_{\text{SR},j}|^2\} + \mathbb{E}_{\{\mathbf{g}, \mathbf{n}_R\}} \{\|\mathbf{w}_k^H \mathbf{n}_R\|^2\}} \quad (6)$$

$$\text{SINR}_{\text{RD},k} = \frac{|\mathbb{E}_{\{\mathbf{g}\}} \{\mathbf{g}_{\text{RD},k}^T \mathbf{a}_k\}|^2}{\text{Var}_{\{\mathbf{g}\}} (\mathbf{g}_{\text{RD},k}^T \mathbf{a}_k) + \sum_{j=1, j \neq k}^K \mathbb{E}_{\{\mathbf{g}\}} \{|\mathbf{g}_{\text{RD},k}^T \mathbf{a}_j|^2\} + \sigma_w^2}. \quad (7)$$

A. Delay Constrained Achievable Rate

To achieve reliable communication at a rate given in (9), the code word length needs to grow without bound. In principle, this implies infinite delay in decoding. While some applications can afford long delays so that (9) is a reasonable approximation, e.g. in URLLC [16] the delay is very short so that the previous rate calculations yield inaccurate results.

With the above in mind, for delay sensitive applications we replace the $R_{*,k}$ in (8) by the finite block length rate [22]

$$R_{*,k}^\tau = R_{*,k} - \sqrt{\frac{V}{\tau}} Q^{-1}(\epsilon) + \frac{\log_2 \tau}{2\tau},$$

where $Q^{-1}(x)$ denotes the inverse of the Q-function. The variable V is so-called channel dispersion and given for the system under consideration by [22]

$$V = \frac{\text{SINR}_{*,k} (2 + \text{SINR}_{*,k})}{(1 + \text{SINR}_{*,k})^2} (\log_2 e)^2,$$

since (5) represents the capacity of an AWGN channel. The code word length is the same as decoding delay and constrained to be $\tau < T - 2K$, that is, the decoding has to be carried out within one coherence block. For simplicity, in the numerical results we set the target error probability ϵ to be equal for the S→R and R→D links. Given the desired E2E decoding error is ϵ_{SD} , the code word error probability over one channel is simply $\epsilon = 1 - \sqrt{1 - \epsilon_{\text{SD}}}$.

IV. NOVEL POWER ALLOCATION SCHEME

Since the power of quantization noise depends on the level of residual LI before digital cancellation is carried out, the relay needs to adjust the transmit power by taking into account the effects of the transmit-side noise and quantization at the receive-side. This can be achieved by taking advantage of the analysis carried out in the previous section.

As shown in (8), the E2E rate depends on the weaker link. Therefore, we propose adjusting the link-wise powers $\{q_1, q_2, \dots, q_K\}$ so that $\text{SINR}_{\text{SR},k} = \text{SINR}_{\text{RD},k}$ for all $k = 1, 2, \dots, K$. This can be achieved via a simple iterative algorithm that allocates power

$$q_k^{(l)} = \frac{\frac{M_t - K}{M_t - K} \rho_{\text{S},k} \hat{\beta}_{\text{SR},k} (\tilde{\beta}_{\text{RD},k} q_{\text{tot}}^{(l-1)} + \sigma_w^2)}{\hat{\beta}_{\text{RD},k} (\sum_{j=1}^K \rho_{\text{S},j} \tilde{\beta}_{\text{SR},j} + \frac{1}{\theta^2} \sigma_{\text{R}}^2)}, \quad (11)$$

to the k th link at the l th iteration. The variable $q_{\text{tot}}^{(l-1)} = \sum_k q_k^{(l-1)}$ is the total transmit power of the relay station in the $(l-1)$ th iteration. The initial point for the iterations (11) can be obtained by assuming that the large scale fading factors of

all terminals are the same and setting $q_1^{(0)} = q_2^{(0)} = \dots = q_K^{(0)}$. Note that the proposed power allocation scheme uses only statistical information so that the power allocation needs to be updated only when the channel statistics change. The algorithm also converges fast, typically within 30 iterations.

V. ENERGY EFFICIENCY

In this paper, the energy consumed by the source and destination terminals is neglected and the energy efficiency for FD relaying is defined as

$$\text{EE} = \frac{C}{E_{\text{tot}}} T,$$

where E_{tot} denotes the average total energy consumption of the relay during one coherence block and is given by

$$E_{\text{tot}} = K P_{\text{Rx,tot}} + \frac{K M_t}{M_r} P_{\text{Rx,tot}} + (T - 2K) (P_{\text{Tx,tot}} + P_{\text{Rx,tot}}). \quad (12)$$

The first and second term include the energy consumed by pilot reception on the S→R and the R→D channel, respectively, while the last term denotes the energy consumed by data reception and transmission at the relay.

To evaluate (12), we need to obtain the total power consumption at the receive-side, $P_{\text{Rx,tot}}$, and transmit-side, $P_{\text{Tx,tot}}$, of the relay. At the receive-side, we single out the power consumed by one ADC, P_{ADC} , as in [9] and define the power consumed by the rest of the components in terms of the power $P_{\text{ADC,ref}}$ consumed by a reference N_{ref} -bit ADC

$$P_{\text{Rx,tot}} = M_r (2P_{\text{ADC}} + \eta_{\text{Rx}} P_{\text{ADC,ref}}).$$

The scalar $\eta_{\text{Rx}} > 0$ is a constant that depends on the system architecture. The transmit-side power excluding the power amplifiers (PAs), P_{PA} , is defined similarly

$$P_{\text{Tx,tot}} = M_t \eta_{\text{Tx}} P_{\text{ADC,ref}} + P_{\text{PA}}.$$

The parameter $\eta_{\text{Tx}} > 0$ depends on the architecture and $P_{\text{PA}} = q_{\text{tot}}/\delta$, where δ denotes the efficiency of the PA.

Finally, for $N > 1$ the power consumed by one ADC is assumed to grow exponentially with N according to [23]

$$P_{\text{ADC}} = E_{\text{con}} 2^N f_{\text{samp}}, \quad N \geq 2,$$

where f_{samp} denotes sampling rate and E_{con} depends on the type of ADC, the average of which is around 5 pJ. The power consumed by one-bit ADC is considered to be negligible [24].

For a relay that operates in HD mode, the active transmit- and receive-side power consumption is the same as in the FD mode. When one of the RF chains is not active, it is assumed to be in a sleep mode that consumes half of the corresponding power when active [25].

VI. NUMERICAL RESULTS

The default parameters in the numerical examples are $T = 100$, $K = 10$, $M_r = M_t = 100$, $f_B = 20$ MHz, $N_{\text{ref}} = 2$, $\delta = 10\%$, $E_{\text{con}} = 5$ pJ, and $\sigma_w^2 = -101$ dBm. For the geometric model we choose $r_{\text{SR}} = r_{\text{RD}} = 100$ m, $d_{\text{SR}} = d_{\text{RD}} = 400$ m and the radio propagation model includes path loss with exponent $\alpha = 4$ and log-normal shadowing with zero-mean and 6 dB variance.

The power of residual LI channel after passive and analog mitigation is assumed to be $\beta_R = -90$ dB [2], [4]. Nyquist-rate sampling is used so that $f_{\text{samp}} = 2f_B$. Since transmitters consume typically more power than receivers, we let $\eta_{\text{Tx}} = 3\eta_{\text{Rx}}$. Power constraint $q_{\text{tot}} \leq 23$ dBm is set for the relay. According to the LTE standard, the required EVM range is $[0.08, 0.175]$, so we model the transmit-side hardware imperfections using $\mu_t = \text{EVM}^2$ and select $\text{EVM} = 0.1$.

To avoid near-far problem at the relay station, simple power control based on long-term statistics is applied at the source terminals, i.e., $\rho_{S,k} = \frac{\gamma}{\beta_{\text{SR},k}}$, where γ is a design parameter. We also denote $\bar{\rho}_S = \mathbb{E}\{\rho_{S,k}\}$ for notational simplicity, where the expectation is over the source terminals, locations and shadow fading. Similarly, in channel estimation phase, we set $\rho_{\text{pS},k} = \gamma_{\text{p}}/\beta_{\text{SR},k}$ and $\rho_{\text{pD},k} = \gamma_{\text{p}}/\beta_{\text{RD},k}$, where $\gamma = \gamma_{\text{p}}$ is assumed in the numerical results.

Fig. 2 demonstrates the throughput of the proposed power allocation scheme for two parameter values $\gamma = -100$ dBm ($\bar{\rho}_S = 6.92$ dBm) and $\gamma = -90$ dBm ($\bar{\rho}_S = 16.85$ dBm), that correspond to received signal-to-noise ratio (SNR) of roughly 0 dB and 10 dB, respectively. Clearly, as the relay station operates in FD mode, the proposed power allocation scheme gives the highest throughput. The curves for HD relaying saturate around $N = 4$ (with relay power optimized so that $R_{\text{SR},k} = R_{\text{RD},k}$). For FD relaying with or without proposed power allocation, it is not necessary to use more than 6-bit ADCs for near optimal performance.

The cumulative density functions (CDFs) of q_{tot} for the proposed power allocation scheme are illustrated in Fig. 3 for different resolutions of ADCs. Only the case $\gamma = -100$ dBm is shown ($\gamma = -90$ dBm yields similar results). The CDFs show how the proposed algorithm reduces the transmit power in case of low resolution ADCs to control quantization noise. The relay power constraint is also satisfied in all cases.

Fig. 4 plots the EE vs. the resolution of the ADCs when $\gamma = -100$ dBm. The optimum resolution of ADCs for maximizing the EE for typical range of η_{Rx} is from 4 to 7 bits for both FD and HD. As η_{Rx} increases, the relative energy consumed by components other than the ADCs grows. As a result, the optimum resolution of the ADCs also increases. In all cases, the proposed FD scheme outperforms HD in energy efficiency.

The optimum number of receive antennas at the relay station in terms of EE is investigated in Fig. 5 for $\gamma = -100$ dBm and $\eta_{\text{Rx}} = 10^2$. For low resolution ADCs, the system should employ higher number of receive antennas than transmit antennas ($M_r > M_t$) to maximize EE. This is explained by the relatively low power consumption of the 1 and 3 bit ADCs.

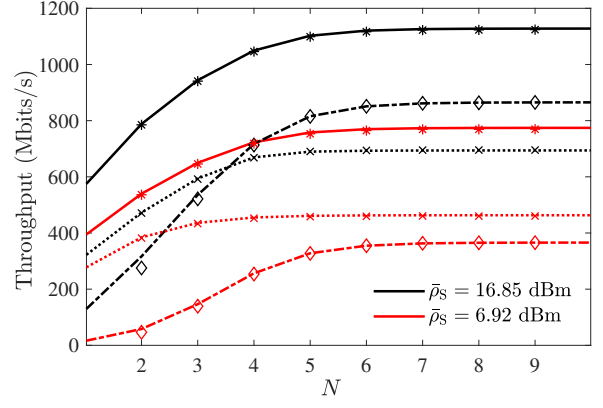


Fig. 2. Throughput of the system vs. the resolution of the ADCs. Analytical results of the proposed power allocation scheme in FD mode (solid), the proposed power allocation scheme in HD mode (dotted) and fixed relay power $q_{\text{tot}} = 23$ dBm in FD mode (dash-dotted) are depicted with curves; Monte Carlo simulations correspond to markers (stars, crosses and diamonds, respectively).

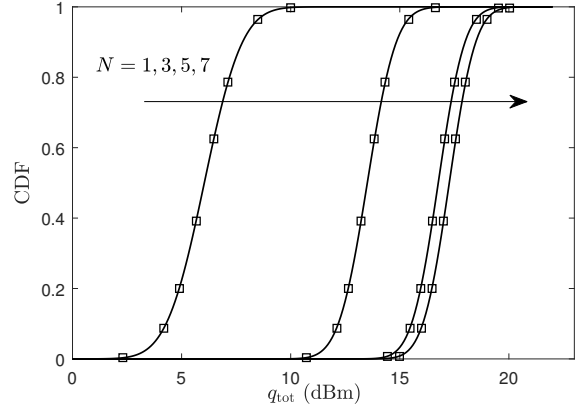


Fig. 3. CDF of the total transmit power at the FD relay station with the proposed power allocation scheme. The empirical CDFs are depicted by the markers; solid lines correspond to Gaussian distribution fitted to the data.

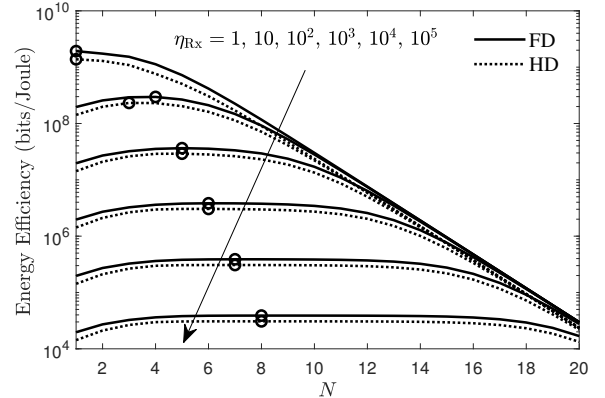


Fig. 4. Energy efficiency vs. ADC resolution N at the relay station. The circles indicate the peaks of the curves. The typical range of the architecture-dependent parameter η_{Rx} is stated to be $[10^2, 10^4]$ in [9].

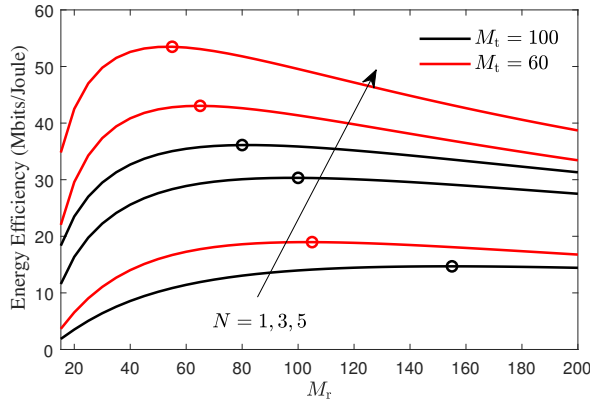


Fig. 5. Energy efficiency vs. the number of receive antennas at the relay with the proposed power allocation scheme. Circle indicates the peak of the curve.

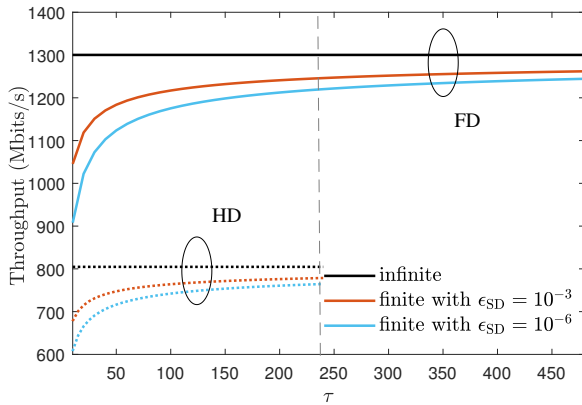


Fig. 6. Throughput vs. code word length τ ; $T = 500$ and $\gamma = -100$ dBm.

Higher resolution $N = 5$ ADCs, on the other hand, consume more power and the opposite ($M_r < M_t$) is true.

Fig. 6 illustrates how fast the system throughput with finite code word length approaches that of the infinite code word length. Since the pilot transmission consumes $2K$ symbols, the code word length with HD and FD relaying cannot exceed $(T - 2K)/2 = 240$ symbols and $T - 2K = 480$ symbols, respectively. It is slightly surprising that the throughput of FD relaying with very strict delay constraint outperforms HD relaying without delay constraint under the given system parameters. This indicates that the proposed FD relaying scheme is a suitable technique for URLLC applications.

VII. CONCLUSION

In this paper, we have analyzed the throughput and energy efficiency of a massive MIMO multipair decode-and-forward FD relaying system with low-resolution ADCs. Based on the analysis, we have proposed a novel power allocation scheme that is aware of the transmit-side hardware imperfections and quantization noise. The proposed scheme aims at maximizing the achievable rate by adjusting the transmit power at the relay on link-by-link basis. The numerical examples demonstrate the benefits of the proposed scheme in improving both the throughput and energy efficiency compared to other considered methods.

REFERENCES

- [1] T. Riihonen, S. Werner, and R. Wichman, "Hybrid full-duplex/half-duplex relaying with transmit power adaptation," *IEEE Trans. Wireless Commun.*, vol. 10, no. 9, pp. 3074–3085, 2011.
- [2] D. Bharadia, E. McMillin, and S. Katti, "Full duplex radios," in *SIGCOMM Comput. Commun. Rev. ACM*, 2013, pp. 375–386.
- [3] H. Q. Ngo *et al.*, "Multipair full-duplex relaying with massive arrays and linear processing," *IEEE J. Sel. Areas Commun.*, vol. 32, no. 9, pp. 1721–1737, 2014.
- [4] A. Sabharwal *et al.*, "In-band full-duplex wireless: Challenges and opportunities," *IEEE J. Sel. Areas Commun.*, vol. 32, no. 9, pp. 1637–1652, Sept. 2014.
- [5] X. Xia *et al.*, "Hardware impairments aware transceiver for full-duplex massive MIMO relaying," *IEEE Trans. Signal Process.*, vol. 63, no. 24, pp. 6565–6580, 2015.
- [6] X. Xiong *et al.*, "Channel estimation for full-duplex relay systems with large-scale antenna arrays," *IEEE Trans. Wireless Commun.*, vol. 15, no. 10, pp. 6925–6938, Oct 2016.
- [7] Z. Chen *et al.*, "Spectral efficiency and relay energy efficiency of full-duplex relay channel," *IEEE Trans. Wireless Commun.*, vol. 16, no. 5, pp. 3162–3175, 2017.
- [8] C. Kong *et al.*, "Full-Duplex massive MIMO relaying systems with Low-Resolution ADCs," *IEEE Trans. Wireless Commun.*, vol. 16, no. 8, pp. 5033–5047, Aug 2017.
- [9] M. Sarajlić, L. Liu, and O. Edfors, "When are low resolution ADCs energy efficient in massive MIMO?" *IEEE Access*, vol. 5, pp. 14837–14853, 2017.
- [10] R. H. Walden, "Analog-to-digital converter survey and analysis," *IEEE J. Sel. Areas Commun.*, vol. 17, no. 4, pp. 539–550, April 1999.
- [11] J. Zhang, L. Dai, S. Sun, and Z. Wang, "On the spectral efficiency of massive MIMO systems with Low-Resolution ADCs," *IEEE Commun. Lett.*, vol. 20, no. 5, pp. 842–845, May 2016.
- [12] L. Fan, S. Jin, C. Wen, and H. Zhang, "Uplink achievable rate for massive MIMO systems with low-resolution ADC," *IEEE Commun. Lett.*, vol. 19, no. 12, pp. 2186–2189, Dec 2015.
- [13] Y. Shim, K. Lee, and H. Park, "Joint relay beamforming design for multilevel nondistributed and distributed amplify-and-forward relay networks," *IEEE Trans. Veh. Technol.*, vol. 66, no. 5, pp. 4443–4448, May 2017.
- [14] A. Mezghani and J. A. Nossek, "Capacity lower bound of MIMO channels with output quantization and correlated noise," in *ISIT 2012*.
- [15] M. Tang, M. Vehkaperä, X. Chu, and R. Wichman, "LI cancellation and power allocation for multipair FD relay systems with massive antenna arrays," *IEEE Wireless Commun. Lett.*, 2019, (in press).
- [16] G. Durisi, T. Koch, and P. Popovski, "Toward massive, ultrareliable, and low-latency wireless communication with short packets," *Proc. IEEE*, vol. 104, no. 9, pp. 1711–1726, 2016.
- [17] S. Wesemann *et al.*, "Measurement and characterization of the temporal behavior of fixed massive MIMO links," in *WSA 2017*.
- [18] E. Björnson *et al.*, "Massive MIMO systems with non-ideal hardware: Energy efficiency, estimation, and capacity limits," *IEEE Trans. Inf. Theory*, vol. 60, no. 11, pp. 7112–7139, 2014.
- [19] A. K. Fletcher *et al.*, "Robust predictive quantization: Analysis and design via convex optimization," *IEEE J. Sel. Topics Signal Process.*, vol. 1, no. 4, pp. 618–632, Dec 2007.
- [20] S. Kay, *Fundamentals of Statistical Signal Processing, Volume I: Estimation Theory*. PTR Prentice-Hall, 1993.
- [21] B. Hassibi and B. M. Hochwald, "How much training is needed in multiple-antenna wireless links?" *IEEE Trans. Inf. Theory*, vol. 49, no. 4, pp. 951–963, Apr. 2003.
- [22] Y. Polyanskiy, H. V. Poor, and S. Verdú, "Channel coding rate in the finite blocklength regime," *IEEE Trans. Inf. Theory*, vol. 56, no. 5, pp. 2307–2359, May 2010.
- [23] J. Jussila and K. Halonen, "Minimization of power dissipation of analog channel-select filter and nyquist-rate A/D converter in UTRA/FDD," in *IEEE Int. Symp. Circuits Syst.*, vol. 4, May 2004, pp. IV–940.
- [24] K. Roth *et al.*, "A comparison of hybrid beamforming and digital beamforming with Low-Resolution ADCs for multiple users and imperfect CSI," *IEEE J. Sel. Topics Signal Process.*, vol. 12, no. 3, pp. 484–498, June 2018.
- [25] G. Auer *et al.*, "How much energy is needed to run a wireless network?" *IEEE Wireless Commun.*, vol. 18, no. 5, pp. 40–49, October 2011.